INSTITUTE OF PHYSICS PUBLISHING PLASMA PHYSICS AND CONTROLLED FUSION

Plasma Phys. Control. Fusion **44** (2002) 423–437 PII: S0741-3335(02)30716-4

H-mode pedestal characteristics and MHD stability of the edge plasma in Alcator C-Mod

D A Mossessian[1], P B Snyder[2], M Greenwald[1], J W Hughes[1], Y Lin[1], A Mazurenko[1], S Medvedev[3], H R Wilson[4] and S Wolfe[1]

[1] MIT, PSFC, Cambridge, MA 02139, USA
[2] General Atomics, San Diego, CA 92186, USA
[3] Keldysh Institute of Applied Mathematics, Russian Academy of Sciences, Moscow, Russia
[4] EURATOM/UKAEA Fusion Association, Culham Science Centre, Abingdon, Oxon OX14 3DB, UK

Received 13 November 2001, in final form 5 February 2002
Published 20 March 2002
Online at stacks.iop.org/PPCF/44/423

Abstract

Under most operational conditions of Alcator C-Mod, the dominant type of H-mode is the steady state enhanced D_α (EDA) mode, characterized by good energy confinement, continuously degraded impurity confinement and absence of regular edge localized modes (ELMs). In this regime, a quasicoherent (QC) electromagnetic mode ($k_\theta \sim 5\,\mathrm{cm}^{-1}$, $f \sim 100\,\mathrm{kHz}$) is observed, localized in the region of the density pedestal. Experimental evidence suggests that the mode is responsible for enhancement of particle transport. It is shown experimentally that the QC mode can exist in a well defined region in edge temperature-safety factor space, favouring high edge q values ($q_{95} \geqslant 3.5$) and requiring moderate pedestal temperature $T_e^{ped} \leqslant T_c$ ($T_c \sim 400\,\mathrm{eV}$). As edge temperature and pressure gradient increase, the QC mode is replaced by broadband low frequency fluctuations ($f < 50\,\mathrm{kHz}$). Small grassy ELMs are observed in these discharges. Analysis of ideal ballooning stability of the C-Mod edge shows that the edge pressure gradient is not limited by infinite n ideal ballooning mode if edge bootstrap current, even reduced by high edge collisionality, is taken into account. Linear stability analysis of coupled ideal peeling/ballooning medium n modes, driven by combination of edge pressure and current gradients, shows that the modes become marginally unstable at C-Mod edge in the range of pressure gradients where the grassy ELMs are observed ($\nabla P \geqslant 1.2 \times 10^7\,\mathrm{Pa\,Wb}^{-1}\,\mathrm{rad}$). This result is consistent with a model of the ELMs as intermediate n peeling/ballooning modes. On the other hand, demonstrated stability of the ideal modes in EDA regime, together with the fact that low T_e^{ped} is required for its existence, supports theoretical models showing resistive character of the QC mode.

Introduction

In the high confinement regime (H-mode) of operation of the tokamak, a transport barrier is formed at the plasma edge. The barrier exhibits itself as a steep pressure gradient in a region which extends over a small fraction of plasma minor radius near the separatrix (so called 'pedestal' region). It has been shown, e.g. in [1, 2], that total confinement and core transport are directly linked to the height and gradient of the temperature and pressure pedestal. Therefore, studying mechanisms that determine the parameters of the pedestal is important for understanding the physics of global plasma confinement.

Large pressure gradients that form in the pedestal region can drive MHD instabilities that limit the pedestal height and, therefore, overall plasma performance. On the other hand, these instabilities provide a relaxation mechanism of the particle transport barrier that is necessary for stationary H-mode operation. Without this relaxation the H-mode usually terminates due to the accumulation of impurities (as in ELM-free H-mode). The most common type of such a relaxation mechanism are edge localized modes (ELMs)—short bursts of enhanced particle and energy transport that intermittently degrade the pedestal. A different regime, with continuously enhanced particle transport across the pedestal but good energy confinement, is observed on C-Mod under most operational conditions. This regime was termed the enhanced D_α (EDA) H-mode because it is often characterized by a strong increase in the intensity of D_α radiation. Associated with this regime is an edge quasicoherent (QC) electromagnetic mode ($f \sim 50$–100 kHz, $\Delta f/f \sim 0.1$). It was shown experimentally that this mode causes enhanced continuous particle transport across the edge barrier, thus leading to a steady state H-mode [3, 4]. It is shown in this paper that the QC mode exists within a well defined region in edge pedestal temperature-safety factor space, favouring high edge q values and requiring moderate T_e^{ped}. At the same time, the pedestal electron pressure profiles, and, therefore, maximum edge pressure gradients, are similar in EDA and ELM-free H-modes under most operational conditions. Infinite n ideal ballooning analysis (n is the toroidal mode number) shows that these gradients are ballooning unstable if no effects of edge bootstrap current driven by pedestal gradients are included. The bootstrap current, even strongly reduced by high C-Mod edge collisionality, modifies the magnetic shear sufficiently to make the pedestal ideal ballooning stable. This picture is similar to the results of stability analysis on DIII-D [5]. However, in contrast to observations made on other machines, DIII-D in particular, no regular type I ELMs were observed on C-Mod when edge pressure gradient exceeds the ideal ballooning limit (calculated without bootstrap current effects) by as much as a factor of 2. Instead, the EDA H-mode is observed at pressure gradient up to 1.5 times the limit, and relatively small grassy ELM-like fluctuations appear to replace the QC mode at higher edge pressure gradient and pedestal temperature.

The purpose of this paper is to summarize the results of the pedestal measurements and MHD stability analysis of Alcator C-Mod edge plasma in order to define operational ranges for observed types of H-mode and determine key plasma parameters that control the H-mode character. In the first section, we summarize the results of pedestal profile measurements for EDA, ELM-free and ELMy regimes and define the operational boundaries of these regimes. The second section, describes the results of ideal MHD stability analysis. Stabilization effects of bootstrap current are analysed. First results of stability analysis of medium n coupled peeling/ballooning modes are presented.

1. Operational range of EDA H-mode

Alcator C-Mod is a compact (major plasma radius $R = 0.68$ m, minor radius $a = 0.22$ m), high field (B_T up to 8 T) tokamak, typically operated with plasma current from 0.6 to 1.2 MA

and average electron densities between 1 and $3 \times 10^{20}\,\mathrm{m}^{-3}$. All discharges described in this paper are obtained in 'standard' shape for C-Mod plasma—a single lower null configuration with lower triangularity around 0.55, upper triangularity near 0.3 and elongation of about 1.65. The toroidal field in all the presented discharges is 5.3 T. The deuterium plasma is heated by the ICRF with H minority heating mechanism using three RF antennas that provide total input power into the plasma of up to 5 MW [24]. In H-mode, the characteristic pressure gradient length in the edge barrier region is typically in the range from 4 to 6 mm. Over this length the electron temperature can change from 20 eV to 1 keV, while the electron density is typically increasing from 0.5 to $2\text{–}3 \times 10^{20}\,\mathrm{m}^{-3}$. A set of dedicated diagnostics has been developed on C-Mod to study edge pedestals. Among them, Thomson scattering measures edge T_e and n_e profiles with $\sim$1 mm resolution within the required dynamic range. The detailed description of the diagnostic can be found elsewhere [6]. Edge reflectometry and phase contrast imaging (PCI) are used to look at edge localized fluctuations [7, 8].

1.1. EDA/ELM-free boundary

In the 'standard' C-Mod operating regime ($I_\mathrm{p} = 0.6\text{–}1.2$ MA, $B_\mathrm{T} = 5.3$ T), with shape parameters described above, two types of H-mode are generally observed—ELM-free and EDA [3, 4]. ELM-free H-mode is characterized by the absence of any kind of edge pedestal relaxation mechanisms and, therefore, by an enhanced impurity confinement. Fast impurity accumulation is evident from the sharply increasing ratio of radiated power to plasma density. Both plasma density and radiated power rise rapidly during an ELM-free H-mode and it terminates in a radiative collapse. In contrast, the EDA H-mode usually exists for as long as the auxiliary heating is applied. It is a steady state regime with constant line average density and radiated power, no significant impurity accumulation throughout the discharge, and energy confinement comparable to that of ELM-free H-mode. The time traces of line average density, midplane D_α intensity, pedestal electron temperature and density and pedestal electron pressure gradient in two typical ELM-free and EDA discharges are shown in figure 1. Values of pedestal T_e and n_e (pedestal height) and maximum pedestal gradient are obtained from edge Thomson scattering by fitting the measured profiles with a hyperbolic tangent function, as described in [6].

The two H-mode discharges presented in the figure were obtained at similar values of target density (line average density in L-mode just prior to the L–H transition), $\bar{n}_{\mathrm{e}0} \sim 1.5 \times 10^{20}\,\mathrm{m}^{-3}$, and input power (net RF power $P_\mathrm{RF} = 2.8$ MW), but different plasma current (0.8 MA for EDA and 1.2 MA for ELM-free). Edge temperature and pressure gradient at the onset of an ELM-free H-mode can reach slightly higher values than in EDA. However, due to fast radiative cooling, the edge temperature drops rapidly leading to decreasing pressure gradient. At the same time impurities continue to accumulate, leading to termination of the H-mode. In EDA H-mode the enhanced impurity transport across the edge barrier is provided by a QC electromagnetic mode localized at the pedestal region [4]. The spectrum of the mode observed by the edge reflectometer diagnostic is shown in figure 1 together with the spectrum of fluctuations in ELM-free phase. The reflectometer channel shown here is tuned to 88 GHz corresponding to a $\sim 1 \times 10^{20}\,\mathrm{m}^{-3}$ reflecting layer density and, therefore, measures the region of plasma in the outer half of the pedestal. The QC mode is clearly seen in EDA as narrow band density fluctuations at $\sim$100 kHz. In contrast, ELM-free H-mode is characterized by lower level of fluctuations over the analysed frequency range relative to L-mode.

Figure 2 compares measured pedestal profiles in EDA and ELM-free H-modes. The profiles represent the discharges shown in figure 1. While there is little difference in electron density pedestal profiles, the temperature pedestal is slightly higher at the beginning of ELM-free H-mode. This is consistent with a generally observed difference in energy confinement between

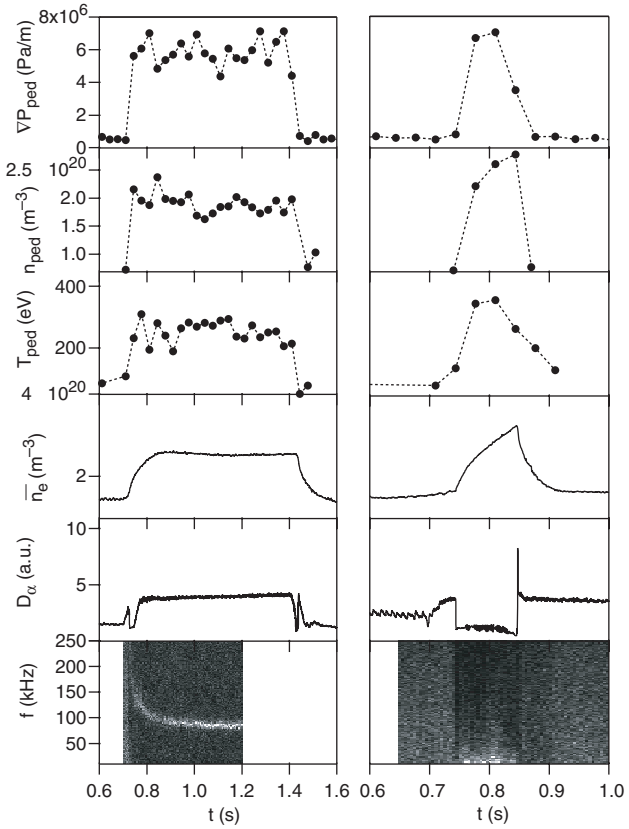

Figure 1. Pedestal parameters in EDA (left) and ELM-free (right) H-mode. The bottom panel shows reflectometer measurements of edge localized fluctuations. The QC mode is clearly seen in the EDA edge.

the two regimes, the confinement in ELM-free H-mode being slightly higher than in EDA. The main difference between the presented discharges is in the value of the edge safety factor q. The value of q at the 95% flux surface is $q_{95} \sim 5$ in the EDA discharge and $q_{95} \sim 3.5$ in ELM-free plasma. Dynamic scans of plasma current and magnetic field have shown that the transition to EDA regime occurs at q_{95} of about 3.5 and higher [3]. At lower values of q_{95} only ELM-free regime can be obtained. The EDA/ELM-free boundary depends also on plasma shape, with EDA occurring at triangularity above 0.35 [4]. In this paper, we present the results obtained at a fixed plasma shape and explore the dependence of the EDA/ELM-free boundary on T_e and n_e pedestal parameters. In particular, a scan of target density was carried out, with the density changing from shot to shot while keeping all other parameters (plasma current i_p, magnetic field B_T and heating power $P_{RF} = 3\,\mathrm{MW}$) fixed. The scan was performed at $i_p = 0.8\,\mathrm{MA}$, corresponding to $q_{95} \sim 5$. On C-Mod, the H-mode pedestal density is set by target density and plasma current, and, at constant I_p, n_e^{ped} changes linearly with $\bar{n}_{e0}$. At line average target densities above $\bar{n}_{e0} \sim 1 \times 10^{20}\,\mathrm{m}^{-3}$, corresponding to pedestal density $n_e^{ped} \sim 1.9 \times 10^{20}\,\mathrm{m}^{-3}$ and higher, EDA H-modes were obtained. Lowering the density pedestal below this value at a constant heating power leads to an increase of the pedestal temperature, T_e^{ped} above ~400 eV, and to a transition to the ELM-free regime with no QC mode observed at the edge. The measured pedestal profiles for ELM-free and EDA H-modes obtained at the same q_{95} value but different

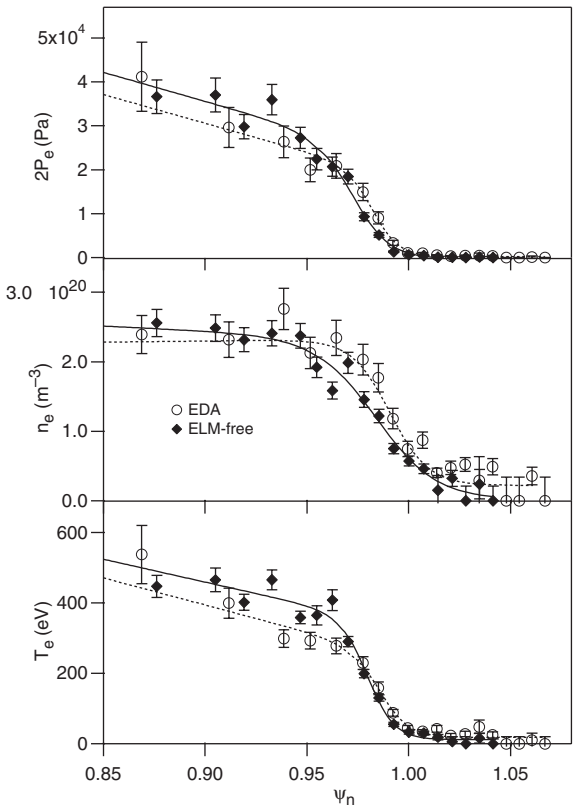

Figure 2. Pressure, density and temperature pedestals in varied q_{95} EDA and ELM-free H-mode. No significant difference in pedestal profiles for two types of H-mode is observed.

target densities are shown in figure 3. It is characteristic for the low density ELM-free discharges that, although temperature and density profiles at the pedestal are very different from EDA H-mode, the maximum pedestal pressure gradient is similar to EDA, providing that the heat source is similar in both discharges. This, combined with similar plasma shape and q profile in those discharges, indicates that the driving term for ideal ballooning instability should be comparable in the EDA and ELM-free plasmas. On the other hand, different T_e and n_e pedestals mean large differences in edge collisionality, leading to substantially different edge bootstrap currents in EDA and ELM-free H-mode. This indicates the important role for the edge current density in ideal MHD. Therefore the ideal MHD stability analysis should include effects of bootstrap current on ballooning stability and current driven edge modes. Also, different pedestal temperatures mean substantially different edge resistivities in these two types of H-modes, which suggests the importance of nonideal effects in edge MHD.

Analysis of the EDA/ELM-free threshold in pedestal density, temperature and safety factor space is complicated by mutual correlations of these parameters. The pedestal density on C-Mod is closely related to the plasma current, and, therefore, to the safety factor. On the other hand, lower pedestal density at constant input power corresponds to higher T_e^{ped}. This correlation of pedestal temperature and density can mask the temperature dependence of the EDA/ELM-free threshold in the experiment when plasma target density (and, therefore, H-mode pedestal density) is scanned at constant q, as discussed in [4]. However, analysis of multiple C-Mod discharges in a wide range of pedestal parameters shows,

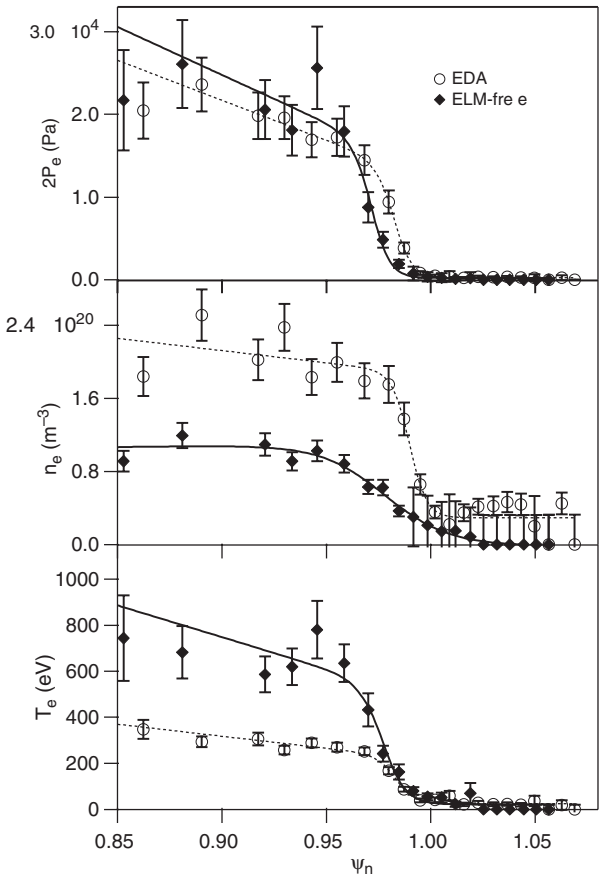

Figure 3. Profiles in EDA and ELM-free H-modes with same q_{95}, different target densities. Note similar pressure gradients in EDA and ELM-free cases.

that the type of H-mode obtained is correlated with pedestal temperature rather than density; in other words the EDA regime can be attained in lower pedestal density discharges with T_e^{ped} below ∼400 eV (low input power shots). The correlation of EDA/ELM-free regimes with edge temperature and q_{95} is summarized in figure 4. Here, the results from an edge database for the latest C-Mod run campaign are presented. Each point on the graph represents a time point in a discharge for which a positive identification of the type of edge fluctuations could be made based on the reflectometer and PCI measurements. The pedestal temperatures are obtained from the hyperbolic tangent fit of measured profiles. The EDA regime generally occurs at low T_e^{ped}, high q values, while ELM-free H-mode can occur in either high q–high T_e^{ped} or low q discharges with any value of edge temperature.

1.2. EDA and ELMy H-modes

Pedestal measurements in high density, high input power ($P_{RF} > 3$ MW) discharges show, that moderate pedestal temperature is a universal condition for the existence of the QC mode associated with EDA H-mode. In the discharges with edge pressure gradients at or above $2\nabla P_e \sim 1.2 \times 10^7$ Pa Wb^{-1} rad, characterized by high values of β, when β_N reaches values of

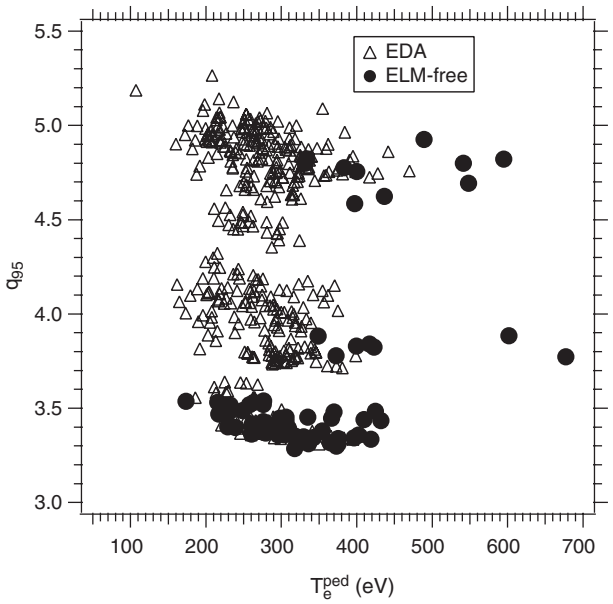

Figure 4. EDA-ELM-free boundary in q_{95}–T_e^{ped} space.

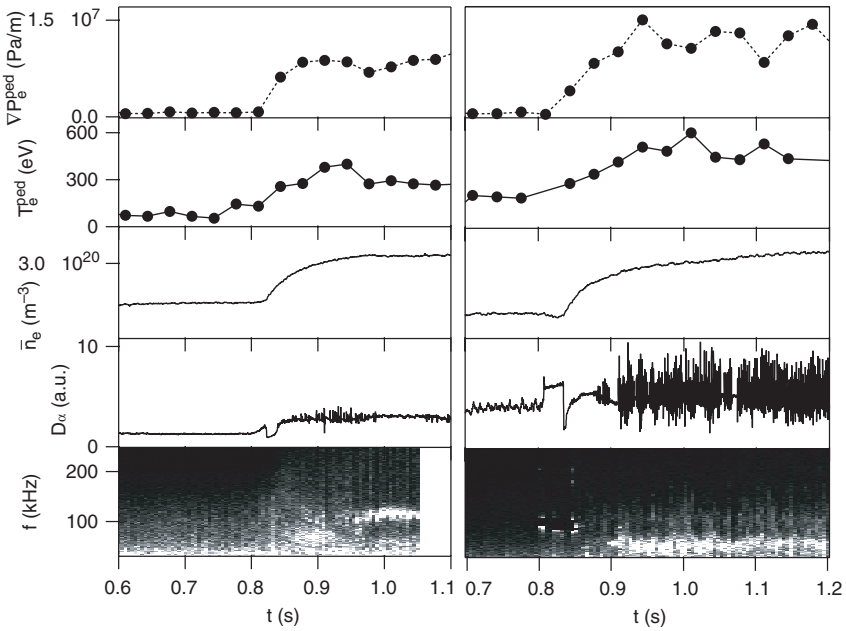

Figure 5. When T_e^{ped} drops below ∼400 eV, ELMs are replaced by the QC mode (left). Higher pedestal temperature and pressure gradient lead to stronger ELMs (right).

1.3 and higher, high frequency ELM-like activity is observed on top of the enhanced level of D_α radiation. Two such discharges are shown in figure 5, one with marginal values of T_e^{ped} and ∇P, where the transition from ELMy to EDA regime is observed, and one with a higher pedestal where purely ELMy H-mode is observed. It is seen from the density fluctuation spectrum

that at high edge pressure gradient, high T_e^{ped} the QC mode is replaced by a low frequency (<50 kHz) broadband turbulence. When pedestal temperature drops below a critical value, the QC mode reappears and the steady state EDA H-mode follows. While T_e^{ped} is high, small ELM-like bursts are seen on top of EDA signal. In the other discharge with higher input power ($P_{RF} = 4.5$ MW) and higher pressure gradient and temperature at the pedestal, larger ELMs are seen in the D_α signal, and the QC mode is not present in the fluctuation spectrum. Since the fluctuations in the D_α signal are well correlated with peaks of the divertor probe saturation current and magnetic coil signals it can be concluded that they represent bursts of particle transport across the pedestal barrier and can be interpreted as ELMs. It should be noted, that during the EDA H-mode the average plasma density remains constant, while in the ELMy regime it is slowly increasing throughout the H-mode, which may indicate a change of the character of the particle transport relative to the EDA regime.

Boundaries between EDA, ELM-free and ELMy H-modes can be identified on a ∇P_e^{ped} versus T_e^{ped} plot presented in figure 6. EDA (identified by the presence of the QC mode at the edge) is limited to the region of low pedestal temperature and pressure gradient. The bulk of ELM-free H-modes cannot be distinguished from EDA in this parameter space, since they were obtained in discharges with similar pedestal characteristics but different magnetic configurations (values of q at the edge). ELM-free H-modes at high pedestal temperature and moderate pedestal gradient are obtained in discharges with low pedestal density and $q_{95} > 3.5$. When ∇P_e^{ped} is pushed higher by increasing the input power in high density discharges, small ELMs replace the QC mode as the pedestal relaxation mechanism.

The disappearance of the QC mode in high power discharges is consistent with the observed dependence of the mode character on T_e^{ped} since at this level of input power the pedestal temperature rises to values above ~400 eV. On the other hand, in contrast to ELM-free discharges, the pedestal density is also high, leading to high ∇P_e^{ped}. Large edge

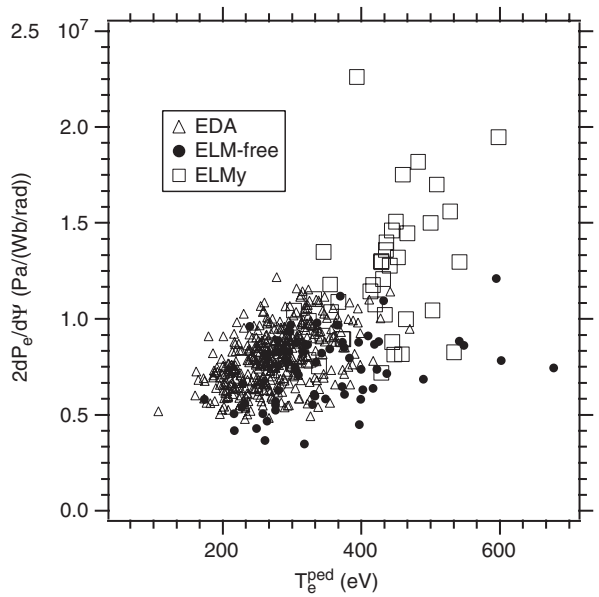

Figure 6. Small ELMs appear in discharges with high pedestal pressure gradient and temperature. Note similar edge pressure gradient range for EDA and ELM-free H-modes.

pressure gradient drives significant edge bootstrap current. At the same time, increasing edge temperature leads to lower collisionality and larger bootstrap fraction at the edge. Although the stability analysis shows that these high pressure gradients remain ballooning stable, the combination of high ∇P and high local current density at the edge can drive coupled peeling/ballooning modes, which exhibit themselves as grassy ELMs observed in the discharges. This hypothesis is discussed in detail in the next section.

The H-modes with small grassy ELMs observed in C-Mod are similar to discharges obtained on JT-60U and ASDEX-U in plasmas with high triangularity and high q. On JT-60U [9], grassy ELMs replace type I ELMs in discharges with $\delta > 0.45$, $q_{95} > 6$ and $\beta_{\mathrm{p}} > 1.6$. The H-modes are steady state, with constant impurity concentration during the grassy ELM phase. In ASDEX-U, grassy ELMs appear in high beta discharges with high triangularity and safety factor, exhibiting similar threshold behaviour in δ and q [10]. In both cases edge pressure gradients are significantly steeper than in the type III ELMy phase, comparable to gradients at the onset of a type I ELM. Recently, observations of an enhanced level of D_α radiation between type I ELMs were reported in high density, high triangularity discharges on JET [11]. The signatures of the observed regime—broadband MHD activity at the edge, high pedestal temperature and pressure—are reminiscent of grassy ELMs observed on other machines.

In all these examples, a combination of strong shaping (high δ) and relatively high q are required to obtain grassy ELMs instead of large, low frequency type I ELMs. At the same time, stability analysis shows that all these discharges are ideal ballooning stable, and, therefore, the observed ELMs cannot be explained in a purely ballooning framework. It was suggested, that ELMs can be represented by moderate to high n instabilities driven by a combination of pressure and current density [12–17]. The suggested mechanism involves an external kink mode, destabilized by increasing edge current density, coupled with an unstable ballooning mode driven by pressure gradient. Due to the coupling with the ballooning mode with larger radial extent, destabilization of the kink mode leads to a large transport event. In this model, the ELM amplitude is determined by the radial extent of the unstable modes. Since modes with higher n (higher k number) will be more radially localized, transition to small ELMs may be explained as a shift of instability to larger n numbers. It was shown in [17] that in JT-60U, $n = 5$–10 modes are unstable in discharges with type I ELMs but stable in high q plasmas with grassy ELMs. If a shift of the instability from lower to higher n is caused by increasing triangularity and q, the transition from large type I ELMs to small ELMs, and the appearance of only small ELMs in high δ, high q C-Mod discharges, can be explained. To explore these questions ideal MHD stability analysis was performed on ELM-free, EDA and ELMy C-Mod discharges for a range of edge parameters.

2. Ideal MHD stability of C-Mod edge

2.1. Infinite n *ideal ballooning stability*

Infinite n ideal ballooning stability of the C-Mod plasma edge was analysed using the BALOO code [18]. The equilibrium configurations for this analysis were obtained with kinetic EFIT based on measured edge pressure profiles. Only electron pressure is measured at the edge and to reconstruct the total pressure profiles two contrasting models were used for the ion temperature profile. The first model is based on the assumption that $T_{\mathrm{i}} = T_{\mathrm{e}}$ over the whole pedestal region. In this case the total pressure is calculated as twice the electron pressure. In the other model, we assume no pedestal in ion temperature and model the T_{i} edge profile as an extension of the core T_{e} profile with the gradient of ion temperature at the edge equal to $\nabla T_{\mathrm{e}}^{\mathrm{core}}$. It turns out, that the total edge pressure gradient calculated in this model is only slightly

(∼15%) lower than $2\nabla P_e^{ped}$ and this difference does not affect the general ballooning stability picture. Besides, this difference is of the order of the experimental errors of measured ∇P. The higher T_i in the pedestal region in the second model leads to lower edge ion collisionality but this has little effect on the edge bootstrap current magnitude, which is determined mainly by electron collisionality [19]. Therefore, in the following section we will concentrate on the results obtained on the assumption of equal T_e and T_i in the pedestal region.

The bootstrap current driven by high edge pressure gradients can significantly alter edge magnetic shear and stabilize ideal ballooning modes even at substantial pressure gradients. Since the magnetic shear is a linear function of the local current, this effect will strongly depend on the magnitude of the bootstrap current in the pedestal region. The current is calculated based on the results of edge T_e and n_e measurements. Since the collisionality at the C-Mod edge is typically rather high ($\nu^* \sim$ 5–50 in the middle of the pedestal) effects of collisionality on bootstrap current have to be taken into account. The edge current for C-Mod stability analysis was calculated as a sum of neoclassical Ohmic current, based on neoclassical resistivity from [19], and the ∇P_e^{ped}-driven bootstrap current. Three models for the bootstrap current were used—a collisionless model based on [20], a model based on neoclassical theory [19] that includes the effects of finite edge collisionality, and a model that assumes total suppression of the bootstrap current by high collisionality.

To achieve the necessary spatial resolution for edge analysis within the 6 mm wide pedestal region, EFIT was run on an 129-point grid, with the edge current density profile constrained to the precalculated values and edge pressure profile input in physical coordinates (r, z) of the Thomson scattering observation volumes relative to the geometrical centre of the machine. The separatrix was fixed in a narrow range (1 mm wide) around the 50 eV electron temperature point, chosen from parallel power balance considerations. Four equilibria based on different C-Mod discharges were analysed. Three analysed equilibria have the same plasma shape and magnetic configuration (q profile) and represent EDA and ELMy discharges, and one has a lower value of q_{95} and represents the ELM-free H-mode. The EDA/ELMy equilibria differ only by edge pressure gradient, one having relatively low $\nabla P_e^{ped} \sim 7 \times 10^6$ Pa Wb^{-1} rad (an EDA H-mode) and two with higher pressure gradient (1.1×10^7 and 1.2×10^7 Pa Wb^{-1} rad) corresponding to the region of transition from EDA to ELMy plasma. For comparison, we chose the low q ($q_{95} = 3.5$) ELM-free equilibrium with highest measured pressure gradient comparable to the ELMy discharge ($\nabla P_e^{ped} \sim 1.2 \times 10^7$ Pa Wb^{-1} rad). While at low ∇P_e^{ped} the infinite n ideal ballooning mode is stable at any bootstrap current, higher edge pressure gradients lead to destabilization of the mode in the model with no bootstrap current. However, when bootstrap current is included in the equilibrium, even strongly reduced by edge collisionality, all discharges are ideal ballooning stable. This result is similar to the stability analysis results from other tokamaks [9–11], and it suggests that the observed edge localized fluctuations (ELMs and QC mode) cannot be modelled in the framework of ideal ballooning theory and it is necessary to include current driven modes.

2.2. *Intermediate* n *coupled peeling/ballooning mode analysis*

The ideal ballooning analysis described above can be considered only as preliminary, since, strictly speaking, the conventional ballooning mode formalism is not valid for analysing the stability of tokamak edge region [12, 13]. It was shown in [12–15] that both pressure gradient and edge current density are important drive mechanisms for the moderate n instabilities, that are likely to control ELM phenomena and pressure gradient limits at the edge. The stability of these modes was analysed with the new general geometry linear MHD stability code ELITE [14, 15] which considers coupled intermediate n ($5 < n < 60$) peeling/ballooning modes

driven by a combination of ∇P^{ped} and j_{boot}. The ELITE runs were based on the same EFIT generated equilibria that were used for ideal ballooning analysis. The results show strong dependence of MHD stability on edge current. In figure 7 the growth rates for modes with $10 < n < 50$ are shown for ELMing discharge with the highest edge pressure gradient for the three models of edge current. For large bootstrap fraction (collisionless model) all the modes considered are unstable with relatively large growth rates, with the fastest growing modes at n around 30. When the effect of collisionality on bootstrap current magnitude is taken into account, modes with lower $n < 15$ become stabilized and the growth rates of higher n modes decreases, with maximum growth rate shifting towards higher n numbers. The assumption of zero bootstrap current leads to further stabilization of the modes, with modes with $n < 35$ being stable (figure 7).

In the model described in the previous section, the ELMs are identified with the current/pressure gradient driven modes, and the amplitude of an ELM is set by the radial extent of the modes, which often becomes smaller as the modes' n numbers increase. The analysis performed on DIII-D showed that large type I ELMs may be identified with the lower n modes ($n < 10$) [21]. On the other hand, these modes are stable in discharges with small, grassy ELMs on JT-60U [17]. Present analysis shows that for the ELMy C-Mod discharge with the expected bootstrap current (collisional model) ELITE calculates the higher n modes ($n > 15$) to be unstable, thus being consistent with the described model of ELMs.

Figure 8 shows growth rates for the mode with $n = 30$ for three discharges with similar plasma shape and magnetic configuration. The growth rates are shown for the three different bootstrap currents modelled. The mode is unstable with growth rate of $\gamma/\omega_{\mathrm{A}} = 0.05$ for expected bootstrap fraction (collisional model) for the maximum pressure gradient ($1.2 \times 10^7\,\mathrm{Pa\,Wb^{-1}\,rad}$), corresponding to the ELMy discharge. For slightly lower

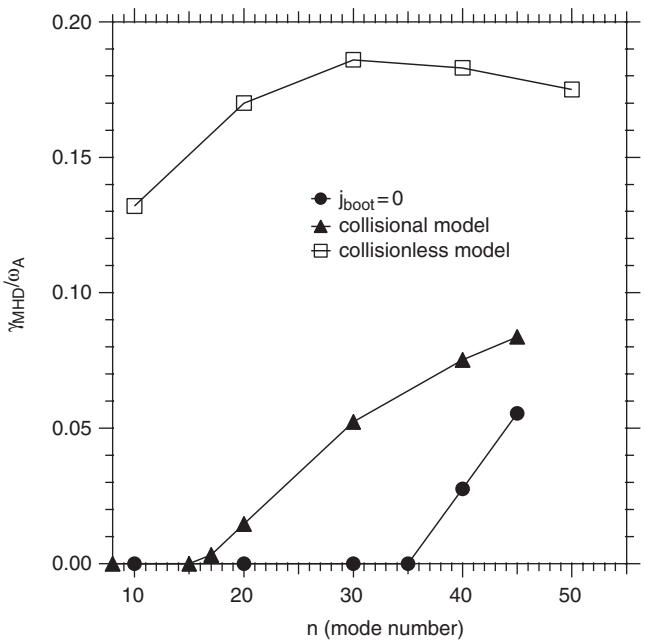

Figure 7. Growth rates of coupled peeling/ballooning modes for an ELMing discharge, using different models for edge bootstrap current. Growth rates are normalized to Alfven frequency, $\omega_{\mathrm{A}} = V_{\mathrm{A}}/R$.

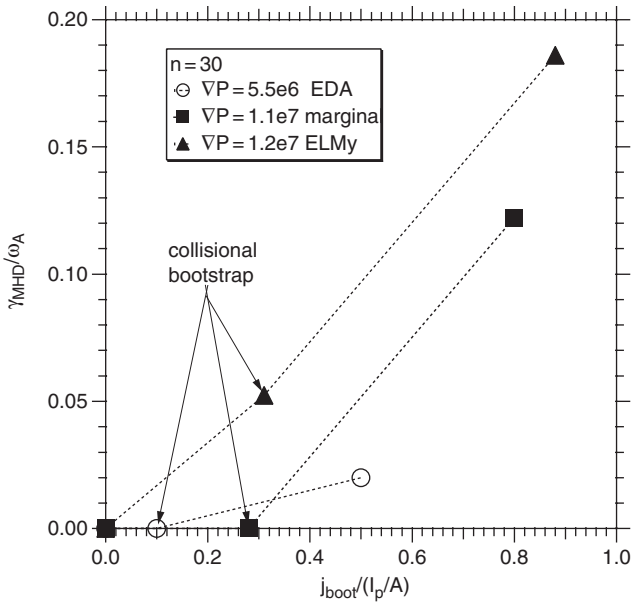

Figure 8. Growth rate of the $n = 30$ mode at different bootstrap fractions for equilibria with increasing pedestal pressure gradient. A: area of plasma cross-section.

$\nabla P_{\rm ped}$ and bootstrap fraction, the mode becomes stable (marginal case with $\nabla P_{\rm ped} = 1.1 \times 10^7$ Pa Wb^{-1} rad) and remains stable for lower pressure gradient EDA H-mode. Although only the $n = 30$ mode is shown in the figure, the ELITE results show that all intermediate n modes are stable in the last two cases. Given the uncertainties in the pressure gradient measurements, equilibrium reconstruction and bootstrap current calculations, we can conclude that intermediate n modes become marginally unstable in the same region of pedestal pressure gradients and temperatures where the transition from EDA to ELMy regime is observed experimentally. The results also indicate that current driven modes are unlikely candidates for explaining the QC mode in EDA regime, since no ideal MHD instability was found in the equilibrium corresponding to the discharge with the QC mode.

Low q ELM-free shots have also been studied, and found to be unstable only to very weak, strongly localized MHD modes, even at large $\nabla P^{\rm ped} = 1.2$ Pa Wb^{-1} rad, similar to the pressure gradients characteristic for ELMing discharges. In figure 9 the radial eigenmode structure of a localized peeling mode from an ELM-free discharge (figure 9(*b*)) is contrasted with the broader structure of the much stronger peeling/ballooning mode in an ELMing discharge (figure 9(*a*)). The absence of an edge relaxation mechanism leading to impurity accumulation in ELM-free H-mode may thus be explained in the framework of the discussed model of ELMs. Although the peeling mode may be unstable, there is no radially extended ballooning structure to provide large enough particle exhaust and no enhancement of particle transport is observed. However, the pedestal relaxation mechanism observed in EDA H-modes that were shown to be ideal MHD stable apparently requires resistive and/or kinetic effects for its description.

A preliminary comparison was performed with the results of the KINX stability code [23], which computes linear ideal MHD growth rates and eigenvectors of axisymmetric plasmas. Since ELITE was run on equilibria limited at the value of the normalized flux $\psi_{\rm N} = 0.985$, to compare with ELITE's results the KINX code was also run on a similarly cut equilibrium. The KINX runs were performed for two cases—the ELMing discharge with collisional edge

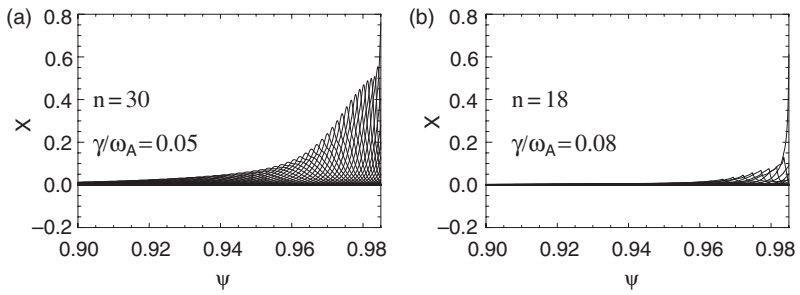

Figure 9. Radial eigenmode structure for $n = 30$ mode in an ELMy discharge (*a*) and for $n = 18$ mode (the n with maximum growth rate) for an ELM-free discharge (*b*).

Table 1. Growth rates of coupled peeling/ballooning modes in 'ELMing' equilibrium resulting from ELITE (1st column), and KINX (2nd column) ideal MHD stability codes.

	ELITE	KINX
$n = 20$	0.0147	0.006
$n = 30$	0.0524	0.056
$n = 40$	0.0752	0.093

bootstrap current and the ELM-free discharge (shown in figure 9). The results of the KINX code for the ELM-free equilibrium show a narrow peeling structure of weakly unstable mode similar to the ELITE run. The comparison of KINX growth rates with the results of ELITE for the ELMing discharge is shown in table 1. The exact values of the growth rates depend strongly on the boundary value of the edge current, which is, strictly speaking, not known, and, for peeling-dominated modes, on the value of the safety factor at the boundary. The differences in the growth rates in the first and second columns of the table could result from differences in the equilibria used for stability calculations, which were cut at slightly different values of ψ_N (0.985 for ELITE and 0.99 for KINX).

Quantitative comparison between the results of different codes would require not only an exact matching of the equilibrium parameters, but also thorough convergence studies including both equilibrium and stability computations. Nevertheless, qualitatively reasonable agreement is seen between growth rates obtained with different stability codes on similar plasma equilibria. The aforementioned trend of increasing growth rate with increasing mode number is also evident from the results of KINX analysis.

The ideal MHD analysis of the C-Mod edge proves to be consistent with the model of ELMs as intermediate n current and pressure gradient driven modes developed in [12–15]. It should be noted, however, that because of large temperature and density gradients in the C-Mod pedestal, the nonideal effects may play an important role in the pedestal stability. Preliminary estimates show that the diamagnetic frequency is comparable to or larger than the maximum calculated growth rates of peeling/ballooning modes for expected bootstrap current even in the ELMing discharge, where the modes are most unstable. This, however, does not necessarily mean that the modes will be stabilized by the diamagnetic effects. The large difference in growth rates between the collisionless and collisional bootstrap cases indicates that the real current may be approaching a threshold where the peeling growth rate increases rapidly, and can increase to the point where it will exceed $\omega*$. The ELM then may be occurring when the kink drive gets strong enough that the kink mode overcomes the FLR stabilization and grows rapidly. Also, it was shown in [22] that when $\omega*$ varies rapidly in the pedestal region

(as is the case in the C-Mod pedestal where the pressure gradient changes considerably over a short radial range), the unstable modes are shifted radially and localize in the regions of smaller diamagnetic frequency. Therefore, no quantitative conclusion about the diamagnetic stabilization of the modes can be made without including the effects self-consistently in the calculations.

3. Conclusions

Pedestal characteristics and their relation to the observed type of H-mode on Alcator C-Mod were studied. It was shown that the QC edge mode associated with the EDA H-mode exists only at moderate pedestal temperature and pressure gradient and is replaced by small ELMs when T_e^{ped} and ∇P^{ped} are increased. In discharges with low pedestal pressure gradient but high pedestal temperature (low density plasmas) the QC mode is not observed, and fast accumulation of impurities in the plasma results from reduced particle transport across the pedestal barrier. Ideal MHD analysis has shown that in EDA H-mode the pedestal is stable to pressure gradient and current driven modes, which, together with the critical dependence of the character of the observed edge modes on pedestal temperature, supports the identification of the QC mode as a resistive ballooning mode. The stability analysis indicates that in ELMing discharges the pedestal parameters are near the point where the ideal kink/peeling growth rate starts increasing rapidly with edge bootstrap current and pressure gradient, in contrast to the EDA and ELM-free cases. This result is consistent with the model of ELMs as coupled peeling/ballooning modes driven by a combination of edge pressure gradient and current density. The fact that the unstable modes in a discharge with experimentally observed small ELMs have relatively high n number ($n > 15$) is also consistent with the model, which describes the ELM as a transport event with magnitude set by the radial extent of the unstable peeling/ballooning mode. However, this conclusion can be considered only as qualitative until the detailed comparison of the intermediate n modes stability is made with the plasmas with large ELMs (as, e.g. on DIII-D tokamak). It is also clear that to study quantitatively the edge localized fluctuations (both ELMs and the QC mode) one needs to consider the diamagnetic effects.

Acknowledgments

We would like to thank R J Hastie for very helpful discussions. This work was supported by D.o.E. Coop. Agreement DE-FC02-99ER54512. H R W is supported by the UK Department of Trade and Industry and EURATOM.

References

[1] Osborne T H *et al* 1998 *Plasma Phys. Control. Fusion* **40** 845
[2] Greenwald M *et al* 1997 *Nuclear Fusion* **37** 793
[3] Greenwald M *et al* 1999 *Phys. Plasmas* **6** 1943
[4] Hubbard A E *et al* 2001 *Phys. Plasmas* **8** 2033
[5] Osborne T H *et al* 2000 *Plasma Phys. Control. Fusion* **42** A175
[6] Hughes J W *et al* 2001 *Rev. Sci. Instrum.* **72** 1107
[7] Lin Y *et al* 1999 *Rev. Sci. Instrum.* **70** 1078
[8] Mazurenko A 2001 *PhD Thesis* Massachusetts Institute of Technology
[9] Kamada Y *et al* 2000 *Plasma Phys. Control. Fusion* **42** A247
[10] Stober *et al* 2001 *Nuclear Fusion* **41** 1123
[11] Saibene G *et al* 2001 *Proc. 28th EPS Conf. on Control. Fusion and Plasma Phys. (Madeira)*
[12] Connor J W, Hastie R J and Wilson H R 1998 *Phys. Plasmas* **5** 2687

[13] Wilson H R *et al* 1999 *Phys. Plasmas* **6** 1925
[14] Snyder P B *et al* 2002 *Phys. Plasmas* at press
[15] Wilson H R *et al* 2001 *Proc. 28th EPS Conf. on Control. Fusion and Plasma Phys. (Madeira)*
Wilson H R *et al* 2002 *Phys. Plasmas* at press
[16] Igitkhanov Yu *et al* 2001 *Proc. 28th EPS Conf. on Control. Fusion and Plasma Phys. (Madeira)*
[17] Lao L L *et al* 2000 *18th IAEA Fusion Energy Conf. (Sorrento)*
[18] Miller R L *et al* 1997 *Phys. Plasmas* **4** 1062
[19] Sauter O and Angioni C 1999 *Phys. Plasmas* **6** 2834
[20] Hirshman S P 1988 *Phys. Fuids* **31** 3150
[21] Ferron J R *et al* 2000 *Phys. Plasmas* **7** 1976
[22] Hastie R J *et al* 2000 *Phys. Plasmas* **7** 4561
[23] Degtyarev L *et al* 1997 *Comput. Phys. Comm*. **103** 10
[24] Wukitch S J *et al* 2001 *Proc. 14th AIP Conf. on Radio Frequency Power in Plasmas* **595** 43